

UCLA

UCLA Previously Published Works

Title

Deposition of 5-Methylcytosine on Enhancer RNAs Enables the Coactivator Function of PGC-1 α

Permalink

<https://escholarship.org/uc/item/10d1k4fz>

Journal

Cell Reports, 14(3)

ISSN

2639-1856

Authors

Aguilo, Francesca

Li, SiDe

Balasubramaniyan, Natarajan

et al.

Publication Date

2016

DOI

10.1016/j.celrep.2015.12.043

Copyright Information

This work is made available under the terms of a Creative Commons Attribution-NonCommercial-NoDerivatives License, available at

<https://creativecommons.org/licenses/by-nc-nd/4.0/>

Peer reviewed



Published in final edited form as:

Cell Rep. 2016 January 26; 14(3): 479–492. doi:10.1016/j.celrep.2015.12.043.

DEPOSITION OF 5-METHYLCYTOSINE ON ENHANCER RNAs ENABLES THE COACTIVATOR FUNCTION OF PGC-1 α

Francesca Aguiló^{1,2,*}, SiDe Li^{1,*}, Natarajan Balasubramaniyan^{4,*}, Ana Sancho^{1,2}, Sabina Benko^{1,2}, Fan Zhang⁵, Ajay Vashisht⁶, Madhumitha Rengasamy^{1,2}, Blanca Andino^{1,2}, Chih-hung Chen^{1,2}, Felix Zhou², Chengmin Qian⁷, Ming-Ming Zhou², James A. Wohlschlegel⁶, Weijia Zhang⁵, Frederick J. Suchy⁴, and Martin J. Walsh^{1,2,3,#}

¹Department of Pediatrics, Icahn School of Medicine at Mount Sinai, New York, NY, 10029, USA

²Department of Pediatrics, Structural and Chemical Biology, Icahn School of Medicine at Mount Sinai, New York, NY, 10029, USA

³Department of Pediatrics, Genetics and Genomic Sciences, Icahn School of Medicine at Mount Sinai, New York, NY, 10029, USA

⁴Children's Hospital Research Institute of Colorado, University of Colorado School of Medicine, Aurora, CO, 80045, USA

⁵Department of Medicine, Division of Nephrology, Laboratory of Bioinformatics, Icahn School of Medicine at Mount Sinai, New York, NY, 10029, USA

⁶Department of Biological Chemistry and Institute of Genomics and Proteomics, University of California, Los Angeles, Los Angeles, CA, 90095, USA

⁷Department of Biochemistry, Lin Ka Shing Faculty of Medicine, University of Hong Kong, Hong Kong, PRC

SUMMARY

#Correspondence to: martin.walsh@mssm.edu.

*These authors contributed equally to this work

Publisher's Disclaimer: This is a PDF file of an unedited manuscript that has been accepted for publication. As a service to our customers we are providing this early version of the manuscript. The manuscript will undergo copyediting, typesetting, and review of the resulting proof before it is published in its final citable form. Please note that during the production process errors may be discovered which could affect the content, and all legal disclaimers that apply to the journal pertain.

SUPPLEMENTAL INFORMATION

Supplemental information includes Extended Experimental Procedures, six supplemental figures and two tables and can be found with this article online.

AUTHOR CONTRIBUTIONS

F.A., S.L., N.B., and M.J.W. conceived the idea for this project and wrote the manuscript. A.S. and F.J.S. edited manuscript. F.A., S.L., N.B., A.S., S.B., M.R., B.A. and C-H.C. conducted cell culture and trans-differentiation and re-programming studies. F.A., N.B., A.V., J.A.W., and M.J.W. performed MS studies and/or analyzed proteomic data. F.A., N.B., S.L., and Fe.Z. generated recombinant proteins for binding studies. S.L. and N.B. performed *in vitro* enzyme studies and binding studies. F.A., S.L., and N.B. performed ChIP and/or ChIP-Seq studies and Fa.Z and W.Z. performed bioinformatic analysis. S.L., F.A., and A.S. performed RNA interference studies and immunoblotting. C.Q. and M-M.Z. generated predicted structural models for SETD7/KMT7a specificity for PGC-1 α .

ACCESSION NUMBERS

Sequencing datasets are available at the National Center for Biotechnology Information Gene Expression Omnibus database under accession number GSE57852 and can be accessed as a reviewer at: <http://www.ncbi.nlm.nih.gov/geo/query/acc.cgi?token=shgbsckihrevbmb&acc=GSE57852>

The Peroxisome proliferator-activated receptor-gamma coactivator 1 alpha (PGC-1 α) is a transcriptional co-activator that plays a central role in adapted metabolic responses. PGC-1 α is dynamically methylated and unmethylated at the residue K779 by the methyltransferase SET7/9 and the Lysine Specific Demethylase 1A (LSD1), respectively. Interactions of methylated PGC-1 α [K779me] with the Spt-Ada-Gcn5-acetyltransferase (SAGA) complex, the Mediator members MED1 and MED17, and the NOP2/Sun RNA methyltransferase 7 (NSUN7) reinforce transcription, and are concomitant with the m⁵C mark on enhancer RNAs (eRNAs). Consistently, loss of *Set7/9* and *NSun7* in liver cell model systems resulted in depletion of the PGC-1 α target genes *Pfkl*, *Sirt5*, *Idh3b* and *Hmox2*, which was accompanied with a decrease in the eRNAs levels associated to these loci. Enrichment of m⁵C within eRNA species coincides with metabolic stress of fasting *in vivo*. Collectively, these findings illustrate the complex epigenetic circuitry imposed by PGC-1 α at the eRNA level to fine-tune energy metabolism.

INTRODUCTION

Processes that contribute to a rapid transcriptional response when the biological need for energy arises converge on the Peroxisome proliferator-activated receptor-gamma coactivator 1 alpha (PGC-1 α) (Finck and Kelly, 2006; Knutti and Kralli, 2001; Lin et al., 2005; Lowell and Spiegelman, 2000; Rosenfeld et al., 2006; Scarpulla, 2008). PGC-1 α is a transcriptional co-activator that interacts with selective transcription factors and chromatin-remodeling complexes to modulate the transcription of target genes (Aubert et al., 2009). Since PGC-1 α has a highly conserved and functional RNA recognition motif (RRM) (Monsalve et al., 2000b), interactions with enhancer-associated RNAs (eRNAs), tethering critical proteins to chromatin, could regulate an adaptive metabolic response in an alternative manner (Natoli and Andrau, 2012, Shiekhattar, 2013).

Biological models illustrating the role of epigenetic and post-translational modifications of co-activators and co-repressor as functional signatures for transcriptional activity have emerged (Berger, 2002, 2007; Jenuwein and Allis, 2001; Rosenfeld et al., 2006). PGC-1 α is acetylated by the histone acetyltransferase GCN5 of the Spt-Ada-Gcn5-acetyltransferase (SAGA) complex (Kelly et al., 2009; Lerin et al., 2006), deacetylated by SIRT1 (Nemoto et al., 2005; Rodgers et al., 2005), serine phosphorylated by AKT/PKB (Li et al., 2007), AMPK, p38 MAPK, and GSK3 β (Fernandez-Marcos and Auwerx, 2011), and asymmetrically dimethylated by PRMT1 (Teyssier et al., 2005). These post-translational modifications can occur in an exclusive or combined manner, and may reinforce or diminish the potential of PGC-1 α to co-activate transcription under diverse metabolic conditions (Canto and Auwerx, 2009), resulting in defective control of multiple transcriptional networks (Lerin et al., 2006; Li et al., 2007; Teyssier et al., 2005). On the other hand, lysine methylation by the histone mono-methyltransferase SET7/9, and lysine demethylation by the Lysine Specific Demethylase 1 (LSD1), have been shown to play an important role in non-histone proteins such as p53 and DNMT1 (Chuikov et al., 2004; Esteve et al., 2009; Nicholson and Chen, 2009; Pradhan et al., 2009; Wang et al., 2009).

Chemical modification also occurs on RNA, functioning as a sensor of the metabolic status to influence gene regulatory networks at the epigenetic level (Townsend and Begley, 2012). The

NOL1/NOP2/Sun (*NSun*) domain-containing genes encode the RNA methyltransferases NSUN2 (Misu), NSUN3, NSUN4, NSUN5 (Wbscr20, Wbscr20a), NSUN6 (NOPD1) and NSUN7, that catalyze the methylation of cytosine to 5-methylcytosine (m⁵C). This modification appears to be ubiquitous (Squires et al., 2012), yet its significance is poorly understood. NSUN5 and NSUN7 have been linked to organism lifespan in yeast (Schosserer et al., 2015) and male sterility, respectively (Harris et al., 2007; Khosronezhad et al., 2014). Moreover, *NSun7* is highly expressed during murine embryogenesis where energy needs are considered high (Chi and Delgado-Olguin, 2013). At the molecular level, m⁵C methylation by NSUN2 in tRNAs and within the 3'UTR of the *INK4A* mRNA promotes stability by abrogating RNA cleavage (Khoddami and Cairns, 2013; Tuorto et al., 2012; Zhang et al., 2012) and in non-coding RNA (ncRNAs) controls the processing of vault ncRNAs into small regulatory RNAs (srRNAs) (Hussain et al., 2013). Conversely, combined loss of *NSun2* and *Dnmt2* in mouse genetic models leads to early embryonic lethality through disruption of the protein synthesis pathway because tRNAs loss (Tuorto et al., 2012).

Here, we demonstrate that PGC-1 α is a substrate for both LSD1 and SET7/9. Lysine methylation of PGC-1 α is directed at the residue K779 and appears selectively coupled to eRNAs with increased retention of the Spt-Ada-Gcn5-acetyltransferase (SAGA) complex component CCDC101/SGF29, and Mediator 1 and 17. Loss of *Set7/9* diminished the capacity to retain the SAGA/ Mediator complex, and consequentially diminished the capacity of PGC-1 α to stimulate transcription. Selective ablation of these eRNAs in mouse hepatoma cells and primary hepatocytes corresponded with diminished expression of their associated genes. Therefore, interactions between PGC-1 α and NSUN7 appear to account for the enrichment of m⁵C-modified eRNAs at enhancers of specific target genes, which finetunes RNA polymerase II activity to metabolic cues. Moreover, enrichment of m⁵C within these specific eRNA species coincides with metabolic stress of fasting in liver *in vivo*. We therefore link intergenic and eRNAs with post-translationally modified PGC-1 α and the transcriptional program of an adaptive metabolic response.

RESULTS

Identification of LSD1 substrates

Several protein lysine methyltransferases and demethylases have been identified to have critical roles in non-histone proteins, affecting human pathogenesis (Hamamoto et al., 2015). To identify specific substrates of LSD1 in Hepa 1–6 cells we used short hairpin RNAs (shRNAs) targeting the expression of murine *Lsd1* (Figure 1A) following stable isotope labeling by amino acids in cell culture (SILAC) assay. PGC-1 α was identified among twenty-seven candidate gene products with a spectra profile that had a strong preference for monomethylated and dimethylated lysine 779 (K779me1>K779me2>K779me0) (Figure 1A). To determine if K779 methylation was a specific post-translational modification of PGC-1 α we directed lysine and arginine methyltransferase activities toward the recombinant C-terminus of human PGC-1 α *in vitro*, containing the K779 residue. Results revealed that K779 of PGC-1 α was preferentially methylated by PRMT1 and SET7/9, whereas, G9a, SUV39H1, or PRMT4 failed to methylate this substrate (Figure 1B). Furthermore, we sought to determine if LSD1 could reverse the abundance of [¹⁴C]-methylated PGC-1 α

species on a stoichiometric basis. Hence, we titrated up to three-fold molar equivalent of recombinant LSD1 with SET7/9 and PGC-1 α (Figure 1B), and demonstrated the competing activities between SET7/9 and LSD1 on the C-terminus of PGC-1 α . To determine the efficiency of SET7/9-mediated PGC-1 α [K779] methylation, a constant amount of SET7/9 and ^3H [AdoMet] was incubated with increasing amounts of either wild-type (PGC-1 α [K779]) or mutant synthetic peptides in which K779 was replaced by an arginine (PGC-1 α [K779R]). We found that the reaction rate curve for the wild-type PGC-1 α [K779] was higher than for the mutant PGC-1 α [K779R] peptide (Figure 1C), suggesting that the lysine K779 of PGC-1 α is an efficient and specific substrate for SET7/9. The model structure of the PGC-1 α [K779] peptide accommodated in the catalytic pocket of SET7/9 enzyme is shown in Figure S1A.

Direct interactions with PGC-1 α are shared between SET7/9 and the SWIRM domain of LSD1

To further study the nature of PGC-1 α interaction with LSD1 and SET7/9, we performed binding assays with recombinant proteins corresponding to various C-terminal fragments of PGC-1 α fused to the polyhistidine tag of pET28b, and GST-tagged SET7/9 or the SWIRM domain of LSD1. PGC-1 α directly bound to SET7/9 and the SWIRM domain of LSD1 *in vitro* (Figure 1D) and *in vivo*, as this interaction was also detected in a native cellular context (Figure S1B). To determine the nature of lysine methylation of PGC-1 α we conducted direct *in vitro* methylation reactions with either wild-type or mutant SET7/9 enzyme, and the synthetic peptide PGC-1 α [K779]. Essentially, MS analysis revealed enrichment of a single methylated species after 30 minutes of incubation with the wild-type SET7/9 but not with the mutated recombinant enzyme (Figure 1E). Confirmation of SET7/9 activity was also tested on total native histones (Figure S1C). To examine whether PGC-1 α became methylated *in vivo*, HEK293 cells were transfected with 3XFLAG tagged PGC-1 α and incubated with L-[methyl- ^3H]methionine as a traceable methyl donor. The experiment was performed in the presence or absence of the homocysteine hydrolase inhibitor adenosine dialdehyde (AdOx) that blocks generation of the cellular methyl donor S-adenosyl-methionine (Pless et al., 2008) and in the presence of cycloheximide and chloramphenicol to block protein synthesis. Metabolic labeling with ^{35}S -methionine was used as a control for the inhibition of protein translation in the presence of cycloheximide and chloramphenicol (Figure 1F, *right panel*). Immunoprecipitation of PGC-1 α revealed a ^3H -methyl labeled PGC-1 α product in the absence but not in the presence of AdOx (Figure 1F, *left and middle panel*). To assess the transcriptional activity of PGC-1 α , we used a heterologous promoter fused with the Gal4 DNA-binding domain. Loss of the C-terminus domain of PGC-1 α as well as mutant PGC-1 α [K779R] led to a decrease in the luciferase activity (Figure 1G, *left panel*), which was accompanied with a decrease in the abundance of histone H3 acetylation at the upstream activating sequences (*UAS*) of the GAL4 promoter (Figure 1G, *right panel*).

Enrichment and characterization of the PGC-1 α [K779me] complex

In order to purify the K779 methyl-specific PGC-1 α complex, we used a combination of affinity and immunoaffinity chromatography. Hepa 1–6 cells were incubated with [^{35}S]-methionine and the nuclear extracts were immunoprecipitated with two discrete biotinylated synthetic peptides corresponding to the unmodified C-terminus of human PGC-1 α .

(PGC-1 α [K779]) and a peptide bearing a specific monomethylated K779 (PGC-1 α [K779me1]). The eluted proteins were electrophoretically separated, visualized by fluorography, and the excised bands were subjected to tandem mass spectrometry MS/MS analysis. Methylated PGC-1 α [K779me1] peptide specifically bound to components of the SAGA complex (CCDC101/SGF29, ADA2, ADA3) and Mediator (MED1 and MED17) (Figure 2A). The selectivity of these interactions was tested by peptide pull-down experiments (Figure 2B). Prominent among the proteins identified was CCDC101/SGF29, which was previously described as a tandem Tudor domain containing protein selective for H3K4me2/3 binding in human and *S. cerevisiae* (Bian et al., 2011). We then tested the binding of the recombinant Tudor domain of CCDC101/SGF29 with different peptides corresponding to methylated and unmodified species of the C-terminus of PGC-1 α and found a selective binding for PGC-1 α [K779me1] and PGC-1 α [K779me2]. H3K4me2 was used as a positive control (Figure 2C). Peptide pull-down experiments showed that the Mediator component MED17 selectively bound the methylated PGC-1 α [K779me1] but not the PGC-1 α [K779] peptide in Hepa 1–6 and 3T3L1 cell lines (Figure S2A).

To assess the robustness of these interactions, Hepa 1–6 extracts were subjected to two purification steps on Phosphocellulose P11 and Q Sepharose columns, followed by size fractionation on a preparative Superose 6 column for an initial enrichment of >200 fold for the complex. This enriched preparation was divided and applied to immunoaffinity column composed of a rabbit polyclonal antibody directed against the methylated PGC-1 α [K779me] peptide (Figures S2B–S2E). The eluted proteins were identified using MS analysis and listed alongside the high sensitivity Coomassie blue-stained polyacrylamide gel (Figure 2D). Although the hepatoma Hepa 1–6 cell line with oncogenic properties may provide a distinct composition from the normal hepatocyte, results from published studies illustrated a pool of shared components (Chen et al., 2009; Wallberg et al., 2003). However, several other candidates remained uncharacterized as for example, components of the SAGA complex, as well as some orphaned nuclear pore and RNA processing components as the N⁵cytosine RNA methyltransferase NSUN7 (Figure 2D). Surprisingly, several Mediator components were absent, suggesting that alternative compositions may exist within a native PGC-1 α complex. To assert the authenticity of the interactions we paneled several protein interactions by co-immunoprecipitation experiments (Figure 2E). We further tested the possibility of differential RNA binding by methylated and unmethylated PGC-1 α by RNA immunoprecipitation (RIP). The PGC-1 α [K779me] fraction strongly retained RNAs, which were suspected to be short ncRNAs as they failed to generate any significant signal from oligo dT mediated reverse transcription of polyadenylated RNA species (Figure 2F).

Genomic distribution of PGC-1 α [K779me]

To ascertain the distribution of chromatin-bound PGC-1 α and methylated PGC-1 α [K779me] we performed chromatin immunoprecipitation coupled with massively parallel DNA sequencing (ChIP-Seq). Because of the suspected avidity of our custom antibody (Figures S2B–S2E), the read depth was substantially greater for the PGC-1 α [K779me] than for total PGC-1 α , rendering 9,472 and 2,395 called peaks, respectively, that were associated with a significant overlapped number of genes (Figure 3A). The distribution of peaks for PGC-1 α [K779me] was slightly shifted 5' upstream of the

TSS when compared with total PGC-1 α (Figure 3B), suggesting an accumulation of intergenic peaks nearest the adjacent genetic loci. Overall, the density of PGC-1 α [K779me] enrichment still greatly appeared over the TSS while significant enrichment for both species of PGC-1 α was found at intergenic sites of neighboring genes (Figure 3C). The genomic distribution of peaks shared between the PGC-1 α [K779me] and total PGC-1 α was in concordance with previous published studies done in human HepG2 cells (Charos et al., 2012). Most of the overlapped binding sites resided on the promoters and the intergenic region, although a minority of peaks was also localized to the intragenic and 3' UTR regions (Figure 3D). PGC-1 α target genes associated with gene ontology (GO) categories like positive regulation of transcription, chromatin modification and PI3/AKT/mTOR signaling, among others (Figure 3E). Furthermore, DNA motifs overrepresented in PGC-1 α [K779me] fell into four dominant motif consensus classes, including the TFIID, LXR, NRF2, and the PPAR family of transcription factors (Figure 3F, *left and middle panel*), which were localized in four metabolic genes identified as specific targets of *Pgc-1 α* by knockdown experiments (Figure 3F, *right panel*; Figure S3A): 6-phosphofructokinase (*Pfkl*), Sirtuin 5 (*Sirt5*), Isocitrate dehydrogenase 3 (*Idh3b*) and Heme oxygenase (*decycling*) 2 (*Hmox2*). Thus, depletion of *Pgc-1 α* led to a decrease of *Pfkl*, *Sirt5*, *Idh3b*, and *Hmox2* expression, which was rescued with wild-type PGC-1 α , but not mutated PGC-1 α {K779R}, overexpression. The known PGC-1 α targets *Pepck* and *Mcad* were tested as controls (Figure S3A). The enrichment of PGC-1 α [K779me] at these loci was validated by ChIP-qPCR in control and *Set7/9* knockdown Hepa 1–6 and differentiated C2C12 cells (Figure S3B)

PGC-1 α [K779me] potentiates both the expression of target genes and the corresponding eRNAs associated to these loci

In order to characterize a functional consequence for the methylated species of PGC-1 α , we reprogrammed wild-type and *Set7/9* $-/-$ mouse embryonic fibroblasts (MEFs) to induced hepatocytes (iHeps), using a modified described protocol (Sekiya and Suzuki, 2011) (Figure 4A). For a greater efficiency of hepatocyte transformation, the retroviral expression of *Hnf4a*, *Foxa1* and *Foxa2* was required, as opposed to using a combination of two factors. Note that the reprogramming efficiency of iHeps was not affected upon *Set7/9* loss (Figure S4A). PGC-1 α expression was induced in iHeps even in the absence of *Set7/9* whereas methylated PGC-1 α [K779me] was depleted in the absence of *Set7/9* when compared to the total pool of PGC-1 α (Figures 4B and 4C). Moreover, markers of definitive hepatocyte differentiation, such as *Ntcp* and *Bsep*, and the nuclear receptor *Rxra* became more evident (Figures S4B and S4C) confirming the status of hepatocyte differentiation. As PGC-1 α [K779me] binding was detected at the active enhancers of the PGC-1 α target genes, characterized by an enrichment of H3K27ac and components of the SAGA and Mediator complexes (Creyghton et al., 2010; Kagey et al., 2010), and was found to show stronger retention of ncRNAs, we tested whether we could detect eRNAs associated with these loci. Thus, specific primers for each PGC-1 α [K779me] enriched peak upstream of the associated TSS were designed and used for measuring the transcript abundance. We detected the expression of eRNAs associated to *Pfkl*, *Sirt5*, *Idh3b*, and *Hmox2* genes, which was drastically abolished upon *Set7/9* loss (Figure 4D, *right panel*). The changes in eRNA expression levels strongly correlated with changes in mRNA expression of the nearby genes (Li et al., 2013) (Figure 4D, *left panel*), although the effect was more moderate.

Furthermore, knockdown of *Set7/9* in Hepa and differentiated C2C12 cells was accompanied with a decrease in the binding of PGC-1 α [K779me], MED1, MED17, and CCDC101/SGF29 at the enhancer of these loci (Figure S3B), suggesting that methylated PGC-1 α [K779me] was essential for the recruitment of Mediator and SAGA complexes at the enhancers of the target genes. Next, we infected cells with wild-type and mutant forms of PGC-1 α and showed that only wild type PGC-1 α corresponded with both modest restitution of eRNAs as well as mRNA transcripts corresponding with *Pfkl* and *Sirt5* (Figure S4D), whereas the expression of *Foxm1b*, a marker of hepatocyte identity, was independent of the methylation status of PGC-1 α (Figure S4E).

***Pfkl*-associated eRNA is preferentially bound by methylated PGC-1 α**

We next examined the RNA binding potential of PGC-1 α [K779me] with the *Pfkl*-associated eRNA by RIP-Northernblot (Figure 5A). In both Hepa1–6 and C2C12 cell lines a signal between 0.5–1 kb was abrogated after knockdown of *Set7/9* (Figure 5B). This result was confirmed by qPCR using the previously reported *Dlx-6as* enhancer-associated transcript (*Evf-2*) as a negative control for PGC-1 α transcript selectivity (Figure 5C) (Berghoff et al., 2013; Feng et al., 2006). Furthermore, we sought to test the binding of the *Pfkl* eRNA with PGC-1 α , PGC-1 α [K779me], CCDC101/SGF29 and MED1, and the RNA binding proteins HEXIM and LARP7. Thus, nuclear extracts from NIH3T3 and Hepa1–6 cells were incubated with the RNA probe, and the detected bands were supershifted when PGC-1 α , PGC-1 α [K779me], CCDC101/Sgf29 and MED1 specific antibodies were added. No binding of *Pfkl*-associated eRNA with either HEXIM or LARP7 was detected, demonstrating selectivity for the engineered ncRNA transcript by PGC-1 α and interacting protein subunits (Figure 5D).

NSUN7 promotes PGC-1 α -mediated transcription and corresponds with enrichment of specific enhancer-associated transcripts for *Pfkl*, *Sirt5*, *Idh3b* and *Hmox2*

To gain deeper mechanistic inside of the association between NSUN7 and PGC-1 α [K779me] (Figure 2D), we performed immunoprecipitation assays with specific antibodies against total and methylated PGC-1 α . Western blot of NSUN7 showed that both PGC-1 α and PGC-1 α [K779me] species associated with the NSUN7 (Figure S5A), which was corresponded with a strong nuclear co-localization as demonstrated by immunocytochemistry microscopy (Figure S5B). The staining of NSUN7 was not confined at the nucleolus but at the nuclear periphery, suggesting that the subcellular localization maybe linked to the cell cycle and cellular stress (Frye and Watt, 2006). Furthermore, ChIP experiments showed an overlapped binding between methylated PGC-1 α [K779me] and NSUN7 at enhancers of PGC-1 α target genes (Figures 6A and S5C). Depletion of *NSun7* corresponded with moderately diminished expression of *Pfkl*, *Sirt5*, *Idh3b* and *Hmox2* mRNA, but more abrupt decrease of the associated eRNAs (Figures 6B and S5D–E), suggesting that m⁵C RNA mark affects eRNA stability. Additionally, 5-azacytidine-mediated RNA immunoprecipitation (Aza-IP) experiments showed a decrease of m⁵C abundance upon *NSun7* depletion at the *Pfkl*, *Sirt5*, *Idh3b*, and *Hmox2* eRNAs, indicating that NSUN7 is the primary methyltransferase for these RNA species (Figure 6C and S5F). RIP assays with NSUN7 antibody and m⁵C RNA detection followed by qPCR further confirmed that both stability and presence of the m⁵C mark were contingent on *NSun7*

expression, whereas, *Eyf-2* transcripts were modestly affected (Figure S5G). Moreover, analysis of m⁵C in the *Pfkl* and *Sirt5* eRNAs by Methylamp™ RNA Bisulfite Conversion Kit in Hepa1–6 cells depleted of *NSun7* and/or *Pgc1α* reinforced the hypothesis that eRNAs selectively undergo cytosine modification (Figure 6D).

***In vivo* function of eRNAs and significance of m⁵C RNA modification**

To assess whether the studied eRNAs affected transcription either *in cis* or *in trans* we performed loss of function assays by knockdown of *Pfkl* and *Sirt5*-associated eRNAs. Depletion of *Pfkl* and *Sirt5*-eRNAs was accompanied by a decrease in *Pfkl* and *Sirt5* mRNA levels and protein abundance respectively (Figures 7A–C and S6A–C), suggesting that these eRNAs affected transcription of neighboring genes, therefore they were functioning in *cis*. Next, we asked whether the *Sirt5* eRNA had the capacity to direct a reporter gene by engineering a trans-activation model similar to what was described (Orom et al., 2010). Doxycycline-induced transcription of the *Sirt5* eRNA increased *Sirt5* reporter activity greater than four fold over the control, indicating that *Sirt5* eRNA had enhancer activities toward *Sirt5* expression (Figure 7D). To further evaluate the physiological function of *Sirt5* eRNA, we tested the lysine de-glutarylase activity of SIRT5 upon knockdown of its associated eRNA (Tan et al., 2014). We found that carbamoyl phosphate synthase 1 (CPS1), a specific substrate of SIRT5, was glutarylated upon depletion of *Sirt5* eRNA, leading to an overall diminishment in CPS1 activity (Figures 7E and 7F). Overall these results suggest that eRNAs are important sensors of the metabolic state.

To further assess the global role of m⁵C RNA, we measured *NSun7* and *Sirt1* expression from liver of fasted DBA/2 mice. Results indicated that *NSun7* was elevated upon 18 hours of fasting and corresponded with a global increase of m⁵C RNA (Figure 7G), detected by quantification of the total cytosine pool in RNA not converted by bisulfite treatment. We conclude from these findings that m⁵C enrichment could be a response to changes in all RNA species, inclusive of tRNAs and rRNAs (Figure S6D), reflecting the stability of these RNA species during metabolic stress. Overall, our work uncovers an unexpected function of ncRNAs for PGC-1α-mediated transcription, shaped by pathways that integrate post-translational modification of PGC-1α with eRNAs and NSUN7. We suggest these studies will contribute to an emerging understanding of how dynamically modified eRNAs may influence transcriptional responses to adaptive metabolic stress (Figure 7H).

DISCUSSION

The post-translational modifications of PGC-1α and their influence on its transcriptional activity have been well studied (Fernandez-Marcos and Auwerx, 2011), and they are related with the rapid ability to change protein activity and function in response to metabolic stimuli. In this report, we showed that PGC-1α undergoes lysine methylation and demethylation at K779 mediated by SET7/9 and LSD1, respectively. Understanding the mechanism and the consequences of PGC-1α methylation may lead to a mean to modulate PGC-1α activity and intervene in metabolic diseases. The methylated pool of PGC-1α corresponds with the retention of SAGA and Mediator complexes, a number of RNA

binding proteins, and with the aggregation of ncRNAs, postulating whether this feature of PGC-1 α activity is linked to its control of transcription.

To reveal specific methylated and unmethylated PGC-1 α target genes, we conducted ChIP-Seq studies in Hepa1–6 cells. Our analysis revealed some discrepancies in the number of peaks for PGC-1 α and PGC-1 α [K779me], likely indicating the poor avidity of the commercial antibody used in our ChIP experiments. In contrast, the custom antibody raised against methylated PGC-1 α [K779me] was optimized for ChIP studies and seemed to reflect the depth of coverage of the methylated species over the total PGC-1 α targets. Nonetheless, we were cautious as our interpretation was shape primarily around the PGC-1 α [K779me] ChIP-Seq data. Moreover, results from the GO ranking primarily activating genes involved in positive regulation of transcription validated our approach and confirmed the quality of the data set. Direct knockdown studies combined with ChIP analysis revealed some *bona-fide* targets as *Pfkl*, *Sirt5*, *Idh3b*, and *Hmox2* genes. Although a significant pool of PGC-1 α [K779me] resides within the TSS, we were able to localize a significant binding at enhancer regions that allowed the characterization of eRNAs overlapping those PGC-1 α [K779me] peaks. Thus, complex ncRNA-protein interactions appear consequential to the fidelity of transcription and to the cellular metabolic fate. While the expanded roles of ncRNAs together with RNA-binding, -processing, and -modifying proteins are emerging as regulators of RNA polymerase II-directed transcription (Nagaike et al., 2011), none of the published studies have illustrated a precise mechanism for eRNA function (Natoli and Andrau, 2012). Here, we provide an unexpected concept for metabolic regulation by PGC-1 α corresponding with eRNAs under a methylation specific context. Therefore, in iHep *Set7/9* $-/-$ the expression of these eRNAs was almost abolished. Furthermore, the binding of PGC-1 α [K779me], Mediator and the SAGA component CCDC101/SFG29 at the target genes was drastically decreased upon *Set7/9* knockdown. While the total PGC-1 α pool certainly contains bound RNA the enrichment with PGC-1 α [K779me] suggests a regulatory mode for PGC-1 α post-translational modification. The fact that PGC-1 α utilizes RNA in control of transcription is not unexpected due to its well-conserved RRM and the previously assumed nature of PGC-1 α tightly coupled with RNA processing (Monsalve et al., 2000a). However, the range of RNA bound by PGC-1 α , together with the role of methylated PGC-1 α , provide new insight regarding the RNA species that may be involved with metabolic homeostasis.

Our notion that m⁵C modification of RNA may be coupled with tRNA, poly-adenylated mRNA, and ncRNA stability adds further complexity to a regulatory mechanism imposed through eRNA species as an additional class of ncRNAs. Thus, *NSun7* depletion corresponded with a loss of m⁵C on the *Pfkl*, *Sirt5*, *Idh3b*, and *Hmox2* associated eRNAs. Furthermore, specific PGC-1 α peaks may suggest that eRNA abundance and turnover are altered as a result of the depletion of m⁵C on the measured transcript. However, the molecular basis of this is not yet evident. It is plausible to consider that PGC-1 α may also respond to depleted (or elevated) pools of tRNA charged with amino acids and their corresponding m⁵C status as a means to sensitize transcriptional mechanisms of available amino acid pools that can accommodate or adapt to metabolic states involved with protein production. This is reminiscent of the simple bacterial model system exploiting tryptophan

attenuation of transcriptional elongation (Babitzke, 2004). While we have no specific evidence of such a mechanism for PGC-1 α , previous findings indicate that the majority of substrates for NSUN2, the close homologue of NSUN7, are tRNAs with a distinct population of polyadenylated mRNAs and ncRNAs (Hussain et al., 2013; Khoddami and Cairns, 2013). Moreover, new evidence suggests that the cytosine methyltransferase activity of NSUN5 influences the lifespan in lower eukaryotes by altering rRNA and consequently ribosome stability (Schosserer et al., 2015). Therefore, like their tRNA and rRNA counterparts, the status of eRNAs marked with m⁵C could be in the direct response to metabolic stress and provide a greater opportunity to fine tune responses to these rapid changes through the transcriptional co-activator function of PGC-1 α . This notion is consistent with our results showing that overall m⁵C RNA abundance and *NSun7* expression are altered in liver during fasting *in vivo*, and that SIRT5 deglutarylase activity on CPS1 is disrupted upon *Sirt5* eRNA depletion.

EXPERIMENTAL PROCEDURES

Detailed experimental procedures are provided as extended experimental procedures.

Cell Culture and inducible Hepatocyte Reprogramming

Cell lines used in this study were obtained from American Type Culture Collection (ATCC) and cultured according to the supplier's recommendations. To induce the differentiation of C2C12 myoblasts, confluent cells were cultured in low-serum differentiation medium (DMEM, 2% horse serum, and 1 μ M insulin), and fresh differentiation medium was changed every 24 h. For ChIP and RNA studies $\sim 7 \times 10^7$ cells and 2×10^6 cells were used, respectively. Mouse embryonic fibroblasts (MEFs) were derived from 13.5 days old embryos from wild type and *Set7/9* $-/-$ mice, corresponding to the C57Bl/6 strain background (Kurash et al., 2008). Programming of MEFs into induced hepatocytes was performed essentially as previously described (Sekiya and Suzuki, 2011).

Enhancer-associated RNA depletion with LNA-Gapmers

LNAs targeting murine *Pfkl* and *Sirt5* enhancer-associated RNAs or a scrambled negative control sequence were designed, synthesized, and supplied by Exiqon. Detailed LNA sequences used in the eRNA depletion experiments will be provided upon request.

Enhancer-associated RNA Reporter Assays

The enhancer RNA for the murine *Sirt5* gene was directionally cloned into the pTRE3G Tet-On™ inducible system (Clontech) (see Table S1) according to manufacturer's recommendations. The control *Evf-2* cDNA was also introduced into pTRE3G and used as a negative control. The murine *Sirt5* promoter was generated from mouse Hepa1–6 cell genomic DNA using the primers (forward 5'-TCAGGGACAGAGGAGTCACTTCTC; reverse 5'-CTCTCAGCACCGTGGCCCATGG) and cloned into the pBV-LUC backbone acquired from Addgene. Hepa 1–6 cells were co-transfected with the plasmids described above and luciferase reporter gene assays were conducted as described previously. Induction of eRNA transcription was performed by addition of tetracycline into medium according to manufacturer's instructions (Clontech).

Quantitation of 5' methylcytosine (m⁵C) in RNA

Bisulfite conversion of RNA was analyzed with the EZ RNA Methylation Kit (Zymo Research) according to the manufacturer's recommendations.

Supplementary Material

Refer to Web version on PubMed Central for supplementary material.

ACKNOWLEDGMENTS

We thank Dr. A. Alonso of the Weill-Cornell College of Medicine's Epigenomic Sequencing Core for advice sequencing and library preparation. We thank Dr. B. Bagley of Bioproximity, LLC for service and support for SILAC analysis and tandem MS studies. We thank Drs. S. Sekiya and A. Suzuki for plasmid constructs, and Dr. Y. Zhao (University of Chicago) for advice for testing SIRT5 enzyme function. F.A. is supported by the Catalan Agency for Administration of University and Research (AGAUR) under a Beatriu de Pinos postdoctoral fellowship. This research was supported by Senior Scholar Award in Aging (AG-SS-2482-10) to M.J.W. from the Ellison Medical Foundation, awards HL067099, HL103967, and CA154903 from the NIH to M.J.W and DK084434 from the NIH to F.J.S.

REFERENCES

- Aubert B, Karyotakis Y, Lees JP, Poireau V, Prencipe E, Prudent X, Tisserand V, Garra Tico J, Grauges E, Martinelli M, et al. Search for dimuon decays of a light scalar boson in radiative transitions $Upsilon \rightarrow \gamma A_0$. *Phys Rev Lett.* 2009; 103:081803. [PubMed: 19792717]
- Babitzke P. Regulation of transcription attenuation and translation initiation by allosteric control of an RNA-binding protein: the *Bacillus subtilis* TRAP protein. *Curr Opin Microbiol.* 2004; 7:132–139. [PubMed: 15063849]
- Berger SL. Histone modifications in transcriptional regulation. *Curr Opin Genet Dev.* 2002; 12:142–148. [PubMed: 11893486]
- Berger SL. The complex language of chromatin regulation during transcription. *Nature.* 2007; 447:407–412. [PubMed: 17522673]
- Berghoff EG, Clark MF, Chen S, Cajigas I, Leib DE, Kohtz JD. Ebf2 (Dlx6as) lncRNA regulates ultraconserved enhancer methylation and the differential transcriptional control of adjacent genes. *Development.* 2013; 140:4407–4416. [PubMed: 24089468]
- Bian C, Xu C, Ruan J, Lee KK, Burke TL, Tempel W, Barsyte D, Li J, Wu M, Zhou BO, et al. Sgf29 binds histone H3K4me2/3 and is required for SAGA complex recruitment and histone H3 acetylation. *Embo J.* 2011; 30:2829–2842. [PubMed: 21685874]
- Canto C, Auwerx J. PGC-1alpha, SIRT1 and AMPK, an energy sensing network that controls energy expenditure. *Curr Opin Lipidol.* 2009; 20:98–105. [PubMed: 19276888]
- Charos AE, Reed BD, Raha D, Szekely AM, Weissman SM, Snyder M. A highly integrated and complex PPARGC1A transcription factor binding network in HepG2 cells. *Genome Res.* 2012; 22:1668–1679. [PubMed: 22955979]
- Chen W, Yang Q, Roeder RG. Dynamic interactions and cooperative functions of PGC-1alpha and MED1 in TRalpha-mediated activation of the brown-fat-specific UCP-1 gene. *Molecular cell.* 2009; 35:755–768. [PubMed: 19782026]
- Chi L, Delgado-Olguin P. Expression of NOL1/NOP2/sun domain (Nsun) RNA methyltransferase family genes in early mouse embryogenesis. *Gene expression patterns : GEP.* 2013; 13:319–327. [PubMed: 23816522]
- Chuiikov S, Kurash JK, Wilson JR, Xiao B, Justin N, Ivanov GS, McKinney K, Tempst P, Prives C, Gambelin SJ, et al. Regulation of p53 activity through lysine methylation. *Nature.* 2004; 432:353–360. [PubMed: 15525938]
- Creyghton MP, Cheng AW, Welstead GG, Kooistra T, Carey BW, Steine EJ, Hanna J, Lodato MA, Frampton GM, Sharp PA, et al. Histone H3K27ac separates active from poised enhancers and

- predicts developmental state. *Proc Natl Acad Sci U S A.* 2010; 107:21931–21936. [PubMed: 21106759]
- Esteve PO, Chin HG, Benner J, Feehery GR, Samaranyake M, Horwitz GA, Jacobsen SE, Pradhan S. Regulation of DNMT1 stability through SET7-mediated lysine methylation in mammalian cells. *Proc Natl Acad Sci U S A.* 2009; 106:5076–5081. [PubMed: 19282482]
- Feng J, Bi C, Clark BS, Mady R, Shah P, Kohtz JD. The Evf-2 noncoding RNA is transcribed from the Dlx-5/6 ultraconserved region and functions as a Dlx-2 transcriptional coactivator. *Genes Dev.* 2006; 20:1470–1484. [PubMed: 16705037]
- Fernandez-Marcos PJ, Auwerx J. Regulation of PGC-1alpha, a nodal regulator of mitochondrial biogenesis. *Am J Clin Nutr.* 2011; 93:884S–890S. [PubMed: 21289221]
- Finck BN, Kelly DP. PGC-1 coactivators: inducible regulators of energy metabolism in health and disease. *J Clin Invest.* 2006; 116:615–622. [PubMed: 16511594]
- Frye M, Watt FM. The RNA methyltransferase Misu (NSun2) mediates Myc-induced proliferation and is upregulated in tumors. *Curr Biol.* 2006; 16:971–981. [PubMed: 16713953]
- Hamamoto R, Saloura V, Nakamura Y. Critical roles of non-histone protein lysine methylation in human tumorigenesis. *Nat Rev Cancer.* 2015; 15:110–124. [PubMed: 25614009]
- Harris T, Marquez B, Suarez S, Schimenti J. Sperm motility defects and infertility in male mice with a mutation in Nsun7, a member of the Sun domain-containing family of putative RNA methyltransferases. *Biol Reprod.* 2007; 77:376–382. [PubMed: 17442852]
- Hussain S, Sajini AA, Blanco S, Dietmann S, Lombard P, Sugimoto Y, Paramor M, Gleeson JG, Odom DT, Ule J, et al. NSun2-mediated cytosine-5 methylation of vault noncoding RNA determines its processing into regulatory small RNAs. *Cell Rep.* 2013; 4:255–261. [PubMed: 23871666]
- Jenuwein T, Allis CD. Translating the histone code. *Science.* 2001; 293:1074–1080. [PubMed: 11498575]
- Kagey MH, Newman JJ, Bilodeau S, Zhan Y, Orlando DA, van Berkum NL, Ebmeier CC, Goossens J, Rahl PB, Levine SS, et al. Mediator and cohesin connect gene expression and chromatin architecture. *Nature.* 2010; 467:430–435. [PubMed: 20720539]
- Kelly TJ, Lerin C, Haas W, Gygi SP, Puigserver P. GCN5-mediated transcriptional control of the metabolic coactivator PGC-1beta through lysine acetylation. *J Biol Chem.* 2009
- Khoddami V, Cairns BR. Identification of direct targets and modified bases of RNA cytosine methyltransferases. *Nat Biotechnol.* 2013; 31:458–464. [PubMed: 23604283]
- Khosronezhad N, Colagar AH, Jorsarayi SG. T26248G-transversion mutation in exon7 of the putative methyltransferase Nsun7 gene causes a change in protein folding associated with reduced sperm motility in asthenospermic men. *Reproduction, fertility, and development.* 2014
- Knutti D, Kralli A. PGC-1, a versatile coactivator. *Trends Endocrinol Metab.* 2001; 12:360–365. [PubMed: 11551810]
- Kurash JK, Lei H, Shen Q, Marston WL, Granda BW, Fan H, Wall D, Li E, Gaudet F. Methylation of p53 by Set7/9 mediates p53 acetylation and activity in vivo. *Molecular cell.* 2008; 29:392–400. [PubMed: 18280244]
- Lerin C, Rodgers JT, Kalume DE, Kim SH, Pandey A, Puigserver P. GCN5 acetyltransferase complex controls glucose metabolism through transcriptional repression of PGC-1alpha. *Cell Metab.* 2006; 3:429–438. [PubMed: 16753578]
- Li W, Notani D, Ma Q, Tanasa B, Nunez E, Chen AY, Merkurjev D, Zhang J, Ohgi K, Song X, et al. Functional roles of enhancer RNAs for oestrogen-dependent transcriptional activation. *Nature.* 2013; 498:516–520. [PubMed: 23728302]
- Li X, Monks B, Ge Q, Birnbaum MJ. Akt/PKB regulates hepatic metabolism by directly inhibiting PGC-1alpha transcription coactivator. *Nature.* 2007; 447:1012–1016. [PubMed: 17554339]
- Lin J, Handschin C, Spiegelman BM. Metabolic control through the PGC-1 family of transcription coactivators. *Cell Metab.* 2005; 1:361–370. [PubMed: 16054085]
- Lowell BB, Spiegelman BM. Towards a molecular understanding of adaptive thermogenesis. *Nature.* 2000; 404:652–660. [PubMed: 10766252]

- Monsalve M, Wu Z, Adelmant G, Puigserver P, Fan M, Spiegelman BM. Direct coupling of transcription and mRNA processing through the thermogenic coactivator PGC-1. *Mol Cell*. 2000a; 6:307–316. [PubMed: 10983978]
- Monsalve M, Wu Z, Adelmant G, Puigserver P, Fan M, Spiegelman BM. Direct coupling of transcription and mRNA processing through the thermogenic coactivator PGC-1. *Mol Cell*. 2000b; 6:307–316. [PubMed: 10983978]
- Nagaike T, Logan C, Hotta I, Rozenblatt-Rosen O, Meyerson M, Manley JL. Transcriptional activators enhance polyadenylation of mRNA precursors. *Molecular cell*. 2011; 41:409–418. [PubMed: 21329879]
- Natoli G, Andrau JC. Noncoding transcription at enhancers: general principles and functional models. *Annu Rev Genet*. 2012; 46:1–19. [PubMed: 22905871]
- Nemoto S, Fergusson MM, Finkel T. SIRT1 functionally interacts with the metabolic regulator and transcriptional coactivator PGC-1{alpha}. *J Biol Chem*. 2005; 280:16456–16460. [PubMed: 15716268]
- Nicholson TB, Chen T. LSD1 demethylates histone and non-histone proteins. *Epigenetics*. 2009; 4:129–132. [PubMed: 19395867]
- Orom UA, Derrien T, Beringer M, Gumireddy K, Gardini A, Bussotti G, Lai F, Zytnicki M, Notredame C, Huang Q, et al. Long noncoding RNAs with enhancer-like function in human cells. *Cell*. 2010; 143:46–58. [PubMed: 20887892]
- Pless O, Kowenz-Leutz E, Knoblich M, Lausen J, Beyermann M, Walsh MJ, Leutz A. G9a-mediated Lysine Methylation Alters the Function of CCAAT/Enhancer-binding Protein-{beta}. *J Biol Chem*. 2008; 283:26357–26363. [PubMed: 18647749]
- Pradhan S, Chin HG, Esteve P-O, Jacobsen SE. SET7/9 mediated methylation of non-histone proteins in mammalian cells. *Epigenetics*. 2009; 4:383–387. [PubMed: 19684477]
- Rodgers JT, Lerin C, Haas W, Gygi SP, Spiegelman BM, Puigserver P. Nutrient control of glucose homeostasis through a complex of PGC-1alpha and SIRT1. *Nature*. 2005; 434:113–118. [PubMed: 15744310]
- Rosenfeld MG, Lunyak VV, Glass CK. Sensors and signals: a coactivator/corepressor/epigenetic code for integrating signal-dependent programs of transcriptional response. *Genes Dev*. 2006; 20:1405–1428. [PubMed: 16751179]
- Scarpulla RC. Transcriptional paradigms in mammalian mitochondrial biogenesis and function. *Physiol Rev*. 2008; 88:611–638. [PubMed: 18391175]
- Schlosser M, Minois N, Angerer TB, Amring M, Dellago H, Harreither E, Calle-Perez A, Pircher A, Gerstl MP, Pfeifenberger S, et al. Methylation of ribosomal RNA by NSUN5 is a conserved mechanism modulating organismal lifespan. *Nat Commun*. 2015; 6:6158. [PubMed: 25635753]
- Sekiya S, Suzuki A. Direct conversion of mouse fibroblasts to hepatocyte-like cells by defined factors. *Nature*. 2011; 475:390–393. [PubMed: 21716291]
- Shiekhhattar R. Opening the Chromatin by eRNAs. *Molecular cell*. 2013; 51:557–558. [PubMed: 24034693]
- Sibbritt T, Patel HR, Preiss T. Mapping and significance of the mRNA methylome. *Wiley interdisciplinary reviews RNA*. 2013; 4:397–422. [PubMed: 23681756]
- Squires JE, Patel HR, Nusch M, Sibbritt T, Humphreys DT, Parker BJ, Suter CM, Preiss T. Widespread occurrence of 5-methylcytosine in human coding and non-coding RNA. *Nucleic acids research*. 2012; 40:5023–5033. [PubMed: 22344696]
- Subramanian K, Jia D, Kapoor-Vazirani P, Powell DR, Collins RE, Sharma D, Peng J, Cheng X, Vertino PM. Regulation of estrogen receptor alpha by the SET7 lysine methyltransferase. *Mol Cell*. 2008; 30:336–347. [PubMed: 18471979]
- Tan M, Peng C, Anderson KA, Chhoy P, Xie Z, Dai L, Park J, Chen Y, Huang H, Zhang Y, et al. Lysine glutarylation is a protein posttranslational modification regulated by SIRT5. *Cell Metab*. 2014; 19:605–617. [PubMed: 24703693]
- Teyssier C, Ma H, Emter R, Kralli A, Stallcup MR. Activation of nuclear receptor coactivator PGC-1alpha by arginine methylation. *Genes Dev*. 2005; 19:1466–1473. [PubMed: 15964996]

- Towns WL, Begley TJ. Transfer RNA methyltransferases and their corresponding modifications in budding yeast and humans: activities, predilections, and potential roles in human health. *DNA Cell Biol.* 2012; 31:434–454. [PubMed: 22191691]
- Tuorto F, Liebers R, Musch T, Schaefer M, Hofmann S, Kellner S, Frye M, Helm M, Stoecklin G, Lyko F. RNA cytosine methylation by Dnmt2 and NSun2 promotes tRNA stability and protein synthesis. *Nat Struct Mol Biol.* 2012; 19:900–905. [PubMed: 22885326]
- Wallberg AE, Yamamura S, Malik S, Spiegelman BM, Roeder RG. Coordination of p300-mediated chromatin remodeling and TRAP/mediator function through coactivator PGC-1alpha. *Molecular cell.* 2003; 12:1137–1149. [PubMed: 14636573]
- Wang J, Hevi S, Kurash JK, Lei H, Gay F, Bajko J, Su H, Sun W, Chang H, Xu G, et al. The lysine demethylase LSD1 (KDM1) is required for maintenance of global DNA methylation. *Nat Genet.* 2009; 41:125–129. [PubMed: 19098913]
- Wissmann M, Yin N, Muller JM, Greschik H, Fodor BD, Jenuwein T, Vogler C, Schneider R, Gunther T, Buettner R, et al. Cooperative demethylation by JMJD2C and LSD1 promotes androgen receptor-dependent gene expression. *Nat Cell Biol.* 2007; 9:347–353. [PubMed: 17277772]
- Zhang X, Liu Z, Yi J, Tang H, Xing J, Yu M, Tong T, Shang Y, Gorospe M, Wang W. The tRNA methyltransferase NSun2 stabilizes p16INK(4) mRNA by methylating the 3'-untranslated region of p16. *Nat Commun.* 2012; 3:712. [PubMed: 22395603]

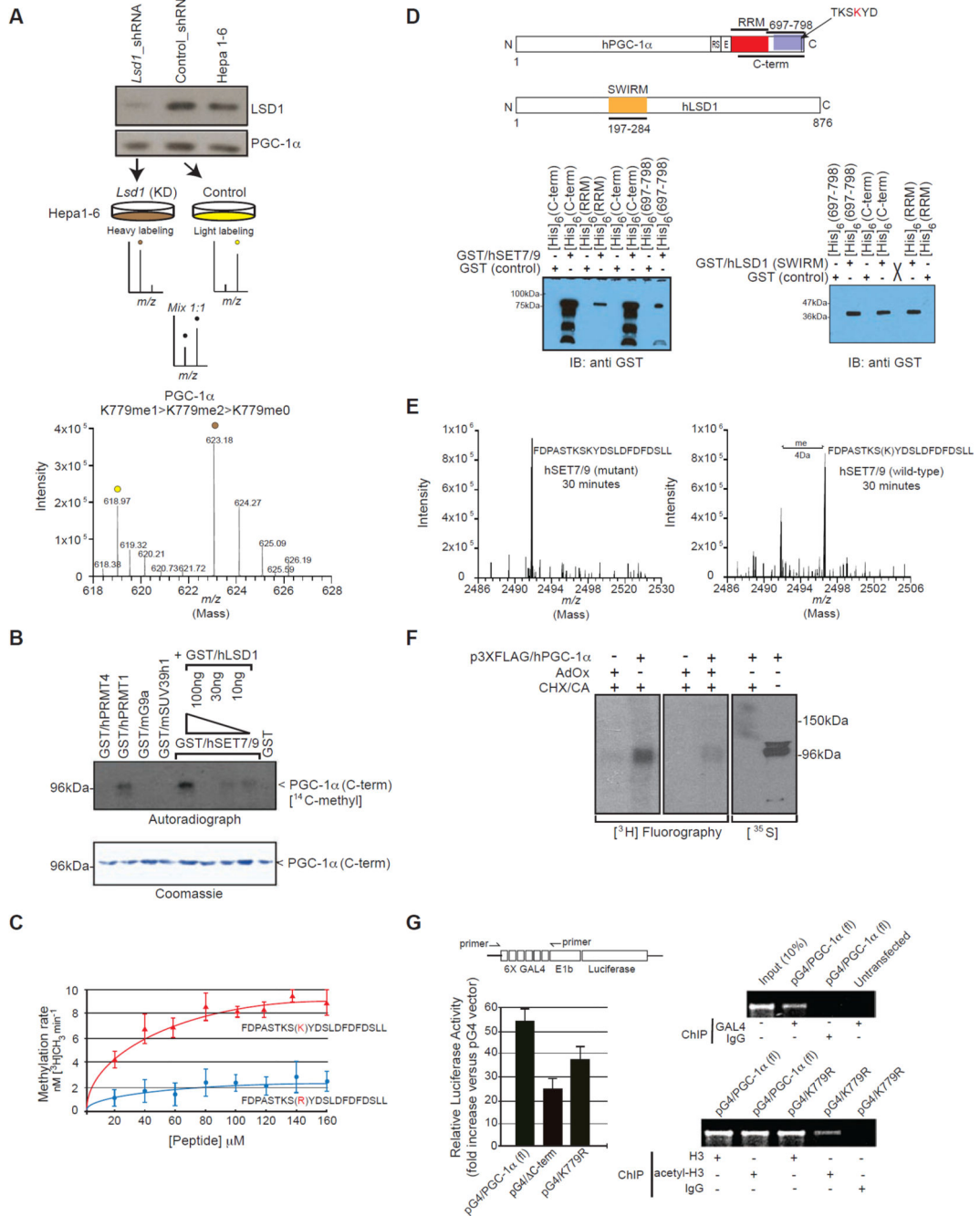


Figure 1. PGC-1α is a direct substrate for LSD1 and SET7/9 and the methylation state is associated with enhanced transcription activation

A) LSD1 and PGC-1α western blot of nuclear extracts from Hepa 1–6 infected with control or *Lsd1* shRNA (upper panel). These nuclear extracts were used for SILAC assays (below). The mass spectra revealed PGC-1α as a significant substrate for LSD1. B) Autoradiography for *in vitro* methylation assays performed with the recombinant C-terminal domain of the human PGC-1α protein and the recombinant methyltransferases indicated in the figure. For the demethylation assay, recombinant C-terminal domain of the human PGC-1α was

incubated with a constant amount of SET7/9 and increased amounts of LSD1. Coomassie staining was used as a loading control (*lower panel*) C) Steady-state kinetic analysis of wild-type PGC-1 α [K779] and mutant PGC-1 α [K779R] peptides for *in vitro* reactions with recombinant SET7/9 enzyme. D) Direct interaction studies of [His]₆-tagged C-terminal domain (C-term), RNA recognition motif (RRM), or amino acids 697 to 798 (697–798) of human PGC-1 α (*as shown in scheme*) with GST-tagged human SET7/9 (*left panel*) or GST-tagged SWIRM domain of human LSD1 (*right panel*). E) MS of the *in vitro* methylation assay of PGC-1 α [K779] synthetic peptide with the wild-type or the catalytically inactive SET7/9 enzyme. F) HEK-293 cells were transfected with triple FLAG-tagged human PGC-1 α and cultured with L-[methyl-³H]methionine, in the presence or absence of adenosine dialdehyde (AdOx), cycloheximide (CHX) and chloramphenicol (CA). Inhibition of translation was monitored by labeling cells with [³⁵S] methionine. After metabolic labeling, 3XFLAG/hPGC-1 α was immunoprecipitated with anti-FLAG M2 beads and visualized by fluorography. G) Schematic diagram illustrating the luciferase-coding gene under the control of Gal4 upstream activating sequences (UAS, pG5luc). The pG5luc reporter construct was transfected with the expression vector encoding wild-type PGC-1 α , the C-terminal deletion of PGC-1 α (C-term) or the mutant PGC-1 α (K779R), fused to the Gal4 DNA binding domain (*left panel*). Luciferase activity was measured 48 h after transfection. ChIP for pan-acetyl H3 and GAL4 was performed in parallel from transfected cultures using primers overlapping the GAL4 UAS (*right panel*).

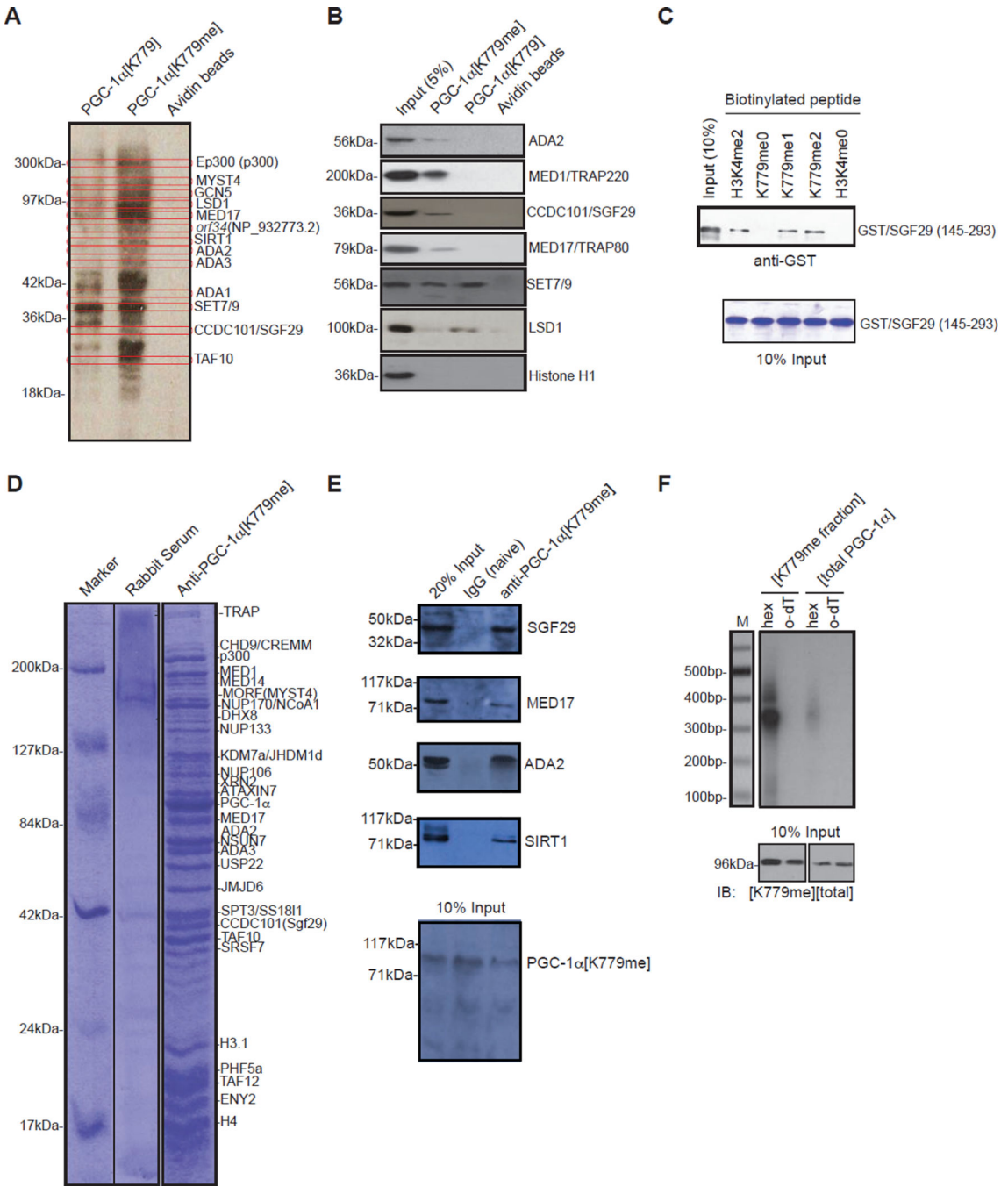


Figure 2. Identification of the nuclear methylated PGC-1α[K779me1] complex

A) Biotinylated PGC-1α[K779] and PGC-1α[K779me1] synthetic peptides were immobilized on avidin beads and incubated with nuclear extracts of Hepa1-6 cells labeled with [³⁵S] methionine. Parallel PAGE was performed and visualized by fluorography or gel bands excised for peptide identification by tandem MS analysis. B) Peptide pull-down of PGC-1α[K779] or methylated PGC-1α[K779me1] peptides with nuclear extracts from Hepa1-6 cells. Immunoblot with specific antibodies are shown. Avidin beads were used as control. C) Peptide pull-down of PGC-1α[K779], PGC-1α[K779me1], PGC-1α[K779me2],

H3K4me0 or H3K4me2 with the GST-tagged tandem tudor domain of the SAGA complex component CCDC101/SGF29 (residues 143–293). Immunoblot with GST antibody (*upper panel*) and coomassie blue staining of the input used (*lower panel*). D) Coomassie blue staining of proteins eluted by anti-PGC-1 α [K779me] immunoaffinity columns. The lanes were sectioned, digested with trypsin, and the extracted peptides were sequenced by mass spectrometry. The positions of molecular mass markers are indicated on the *left*. Naïve rabbit Ig was used as a control shown in the *center* lane. E) Immunoprecipitation with anti-PGC-1 α [K779me] or with naïve Ig serum was performed from Hep1–6 hepatoma cell nuclear extracts and immunoblotted for the indicated interacting partners. Immunoblot of PGC-1 α [K779me] of the 10% of input used in this assay (*lower panel*). F) UV crosslinked RNA was immunoprecipitated with methylated PGC-1 α [K779me] and total PGC-1 α antibodies. The enriched RNA was reverse -transcribed using either oligo-dT (o-dT) or random hexamers primers (hex) and labeled with CTP, [α -³²P]. Input level of methylated PGC-1 α [K779me] and total PGC-1 α is shown *below*.

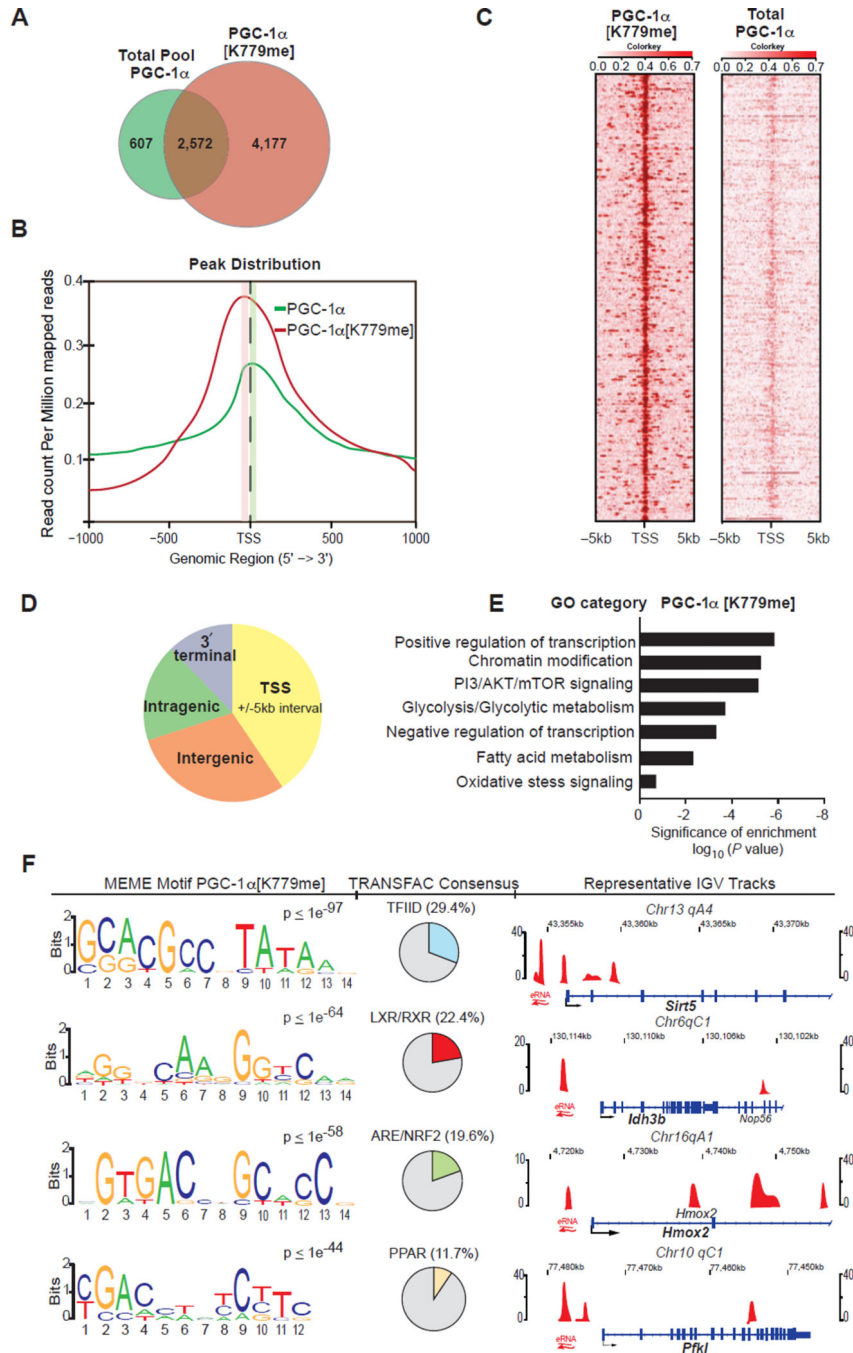


Figure 3. PGC-1α[K779me] is associated with enhancers and core promoters of metabolic genes
 A) Venn diagram representing the overlap of PGC-1α[K779me] and total PGC-1α bound genes. B) Peak distribution of enriched ChIP reads along the annotated transcriptional start sites (TSS) for PGC-1α[K779me] and the total pool of PGC-1α. C) Density alignment of ChIP peaks relative to the TSS for PGC-1α[K779me] and unmethylated PGC-1α. D) Genome distribution of the overlapped peaks. E) Gene ontology analysis of the PGC-1α[K779me] ChIP peaks. F) Motif discovery from summit regions from PGC-1α[K779me] ChIP-seq. MEME analysis significantly identified specific transcription

factor (TF) motifs (left) with their corresponding p values (*top right of motif*); TRANSFAC analysis indicates the proportion of TF motifs found among the overall peak distribution (*center*). Custom IGV tracks of genes represented as sequences enriched for specific TFs derived from the MEME enrichment analysis (*right*).

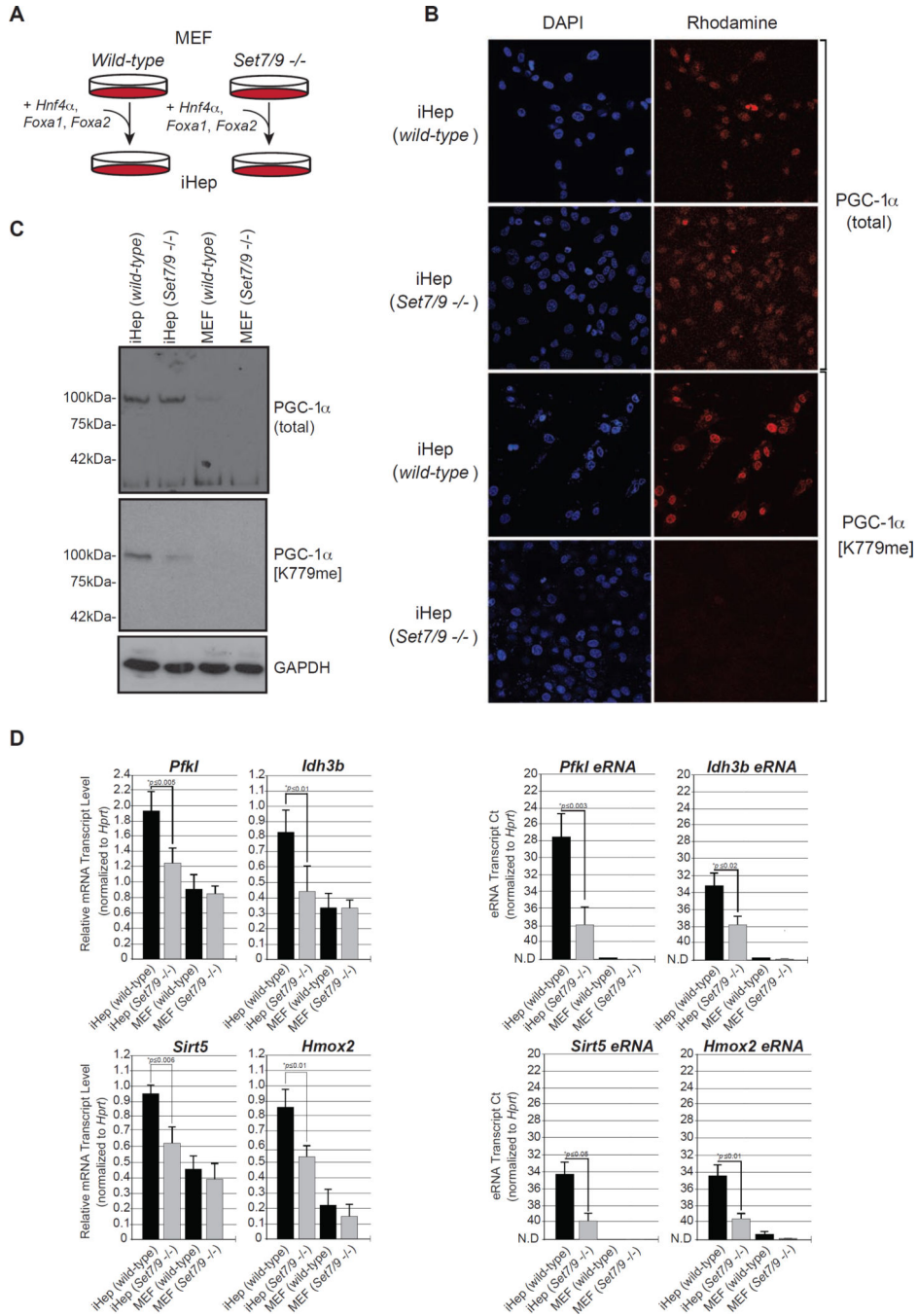


Figure 4. Loss of Set7/9 contributes to eRNAs depletion

A) Schematic diagram illustrating the transdifferentiation protocol of wild-type and *Set7/9* null (*Set7/9* -/-) MEFs into induced hepatocytes (iHeps). **B)** Immunocytochemistry analysis of wild-type and *Set7/9* null iHep, using PGC-1α[K779me] and PGC-1α antibodies and Rhodamine-labeled anti-rabbit IgG (right panel). DAPI was used for DNA staining (left). **C)** Western blot of total PGC-1α and PGC-1α[K779me] in wild-type and *Set7/9* -/- iHep and MEFs, respectively. GAPDH was used as a loading control. **D)** qPCR assays of the *Pfkf*,

Sirt5, *Idh3b*, and *Hmox2* mRNA transcripts (*left panel*) and the associated eRNAs upstream the TSS (*right panel*) in wild type and *Set7/9* $-/-$ iHep and MEFs.

Author Manuscript

Author Manuscript

Author Manuscript

Author Manuscript

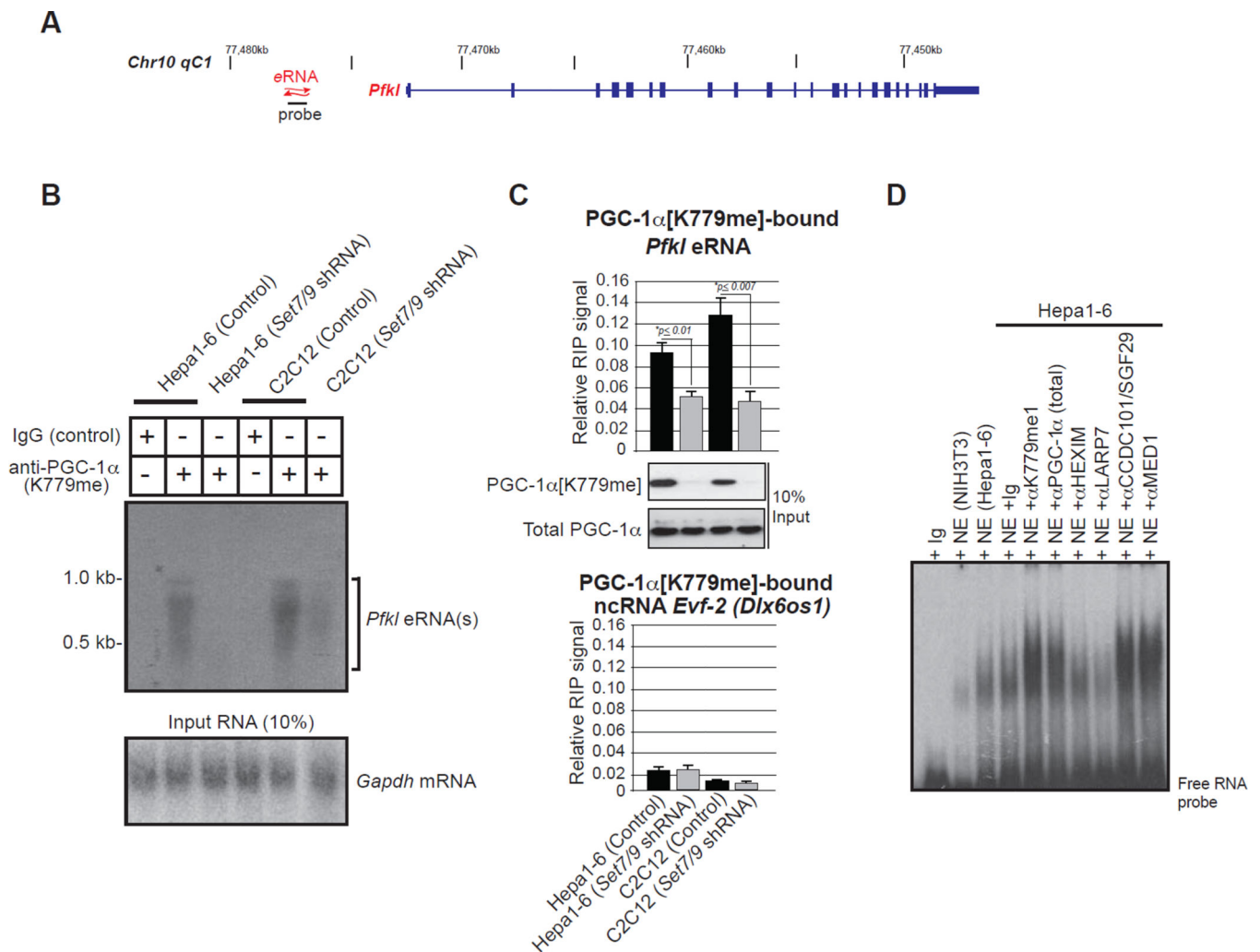


Figure 5. Binding to eRNAs corresponds with the SET7/9-mediated methylated state of PGC-1α
A) Schematic diagram of the murine *Pfk1* locus. The position of the eRNA probe used in different assays is shown. B) Binding of PGC-1α[K779me] to *Pfk1*-associated eRNA was analyzed by RIP Northern blot analysis upon knockdown of *Set7/9* in both Hepa 1–6 and C2C12 cells. Detection of *Gapdh* mRNA was used as a control (lower panel). C) qPCR of the *Pfk1*-associated eRNA and the *Dlx2* enhancer-associated *Evf-2* (*Dlx6os1*) transcript used as a negative control, after RIP with PGC-1α[K779me] antibody upon *Set7/9* depletion in both Hepa 1–6 and C2C12 cells. Shown, are the relative abundance for 10% of total input of PGC-1α as a total and methylated K779 fractions. D) RNA EMSA using Hepa 1–6 nuclear extracts and the radiolabeled RNA probe corresponding to the *Pfk1*-associated eRNA described in A. The indicated antibodies were added to detect supershifted bands.

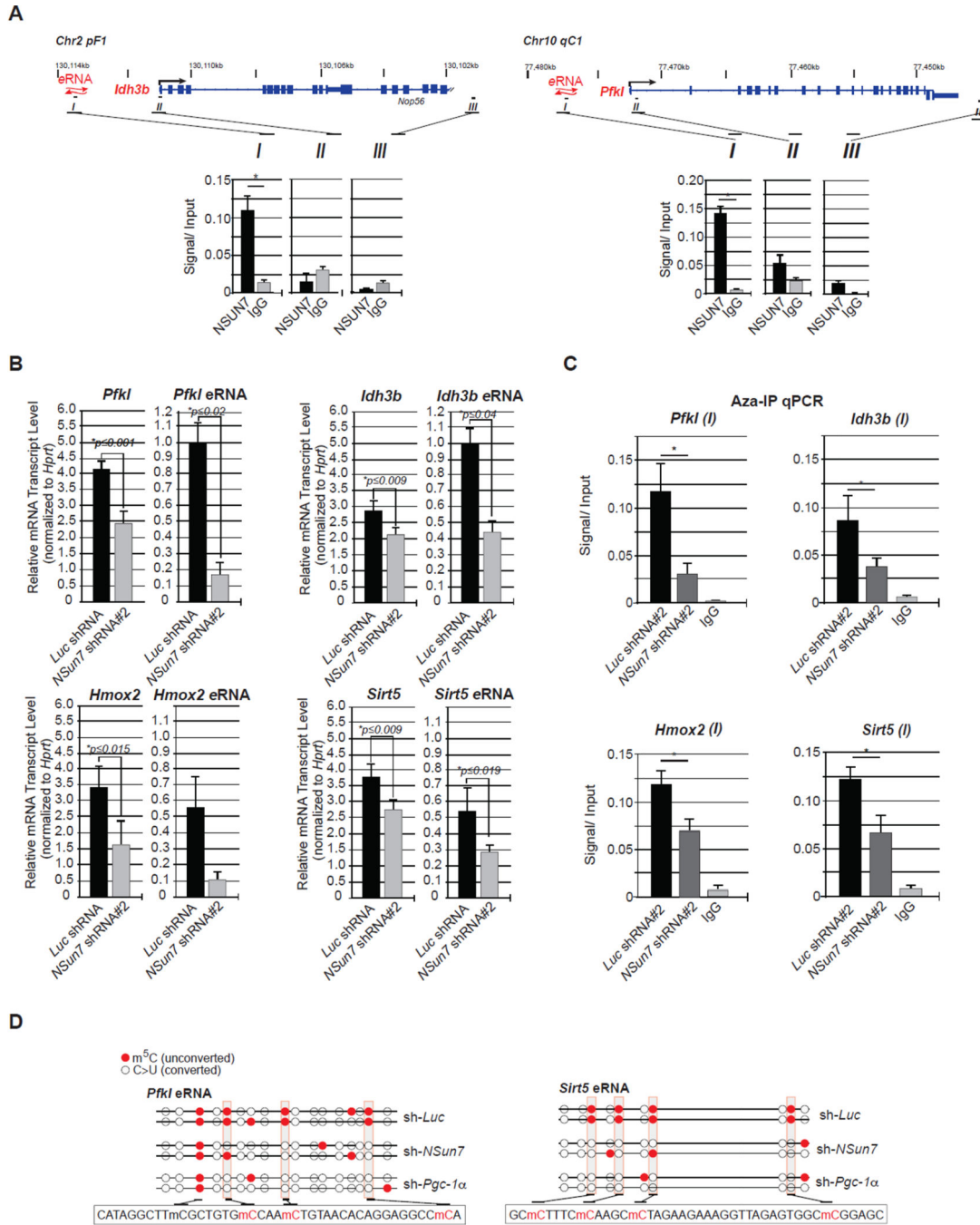


Figure 6. The NSUN7 RNA methyltransferase influences PGC-1 α target gene expression

A) ChIP-qPCR of NSUN7 performed on three discrete regions of the *Pfk1* and *Idh3b* loci as shown in the diagram. B) Knockdown of *NSun7* results in downregulation of *Pfk1*, *Sirt5*, *Idh3b*, and *Hmox2* mRNA and the associated eRNAs. C) qPCR of eRNAs captured by Aza-IP with NSUN7 or IgG control in wild-type and *NSun7* shRNA Hepa1–6 cells. D) Bisulfite conversion identified specific unconverted *N*⁵-methylcytosine in the *Pfk1* and *Sirt5* eRNAs dependent on the presence of NSUN7 and mediated through PGC-1 α . Hepa1–6 were

depleted of *Pgc1 α* and *NSun7* by shRNA and the total RNA was subjected to bisulfite treatment. Two individual biological replicates as total RNA were analyzed ($n=2$).

Author Manuscript

Author Manuscript

Author Manuscript

Author Manuscript

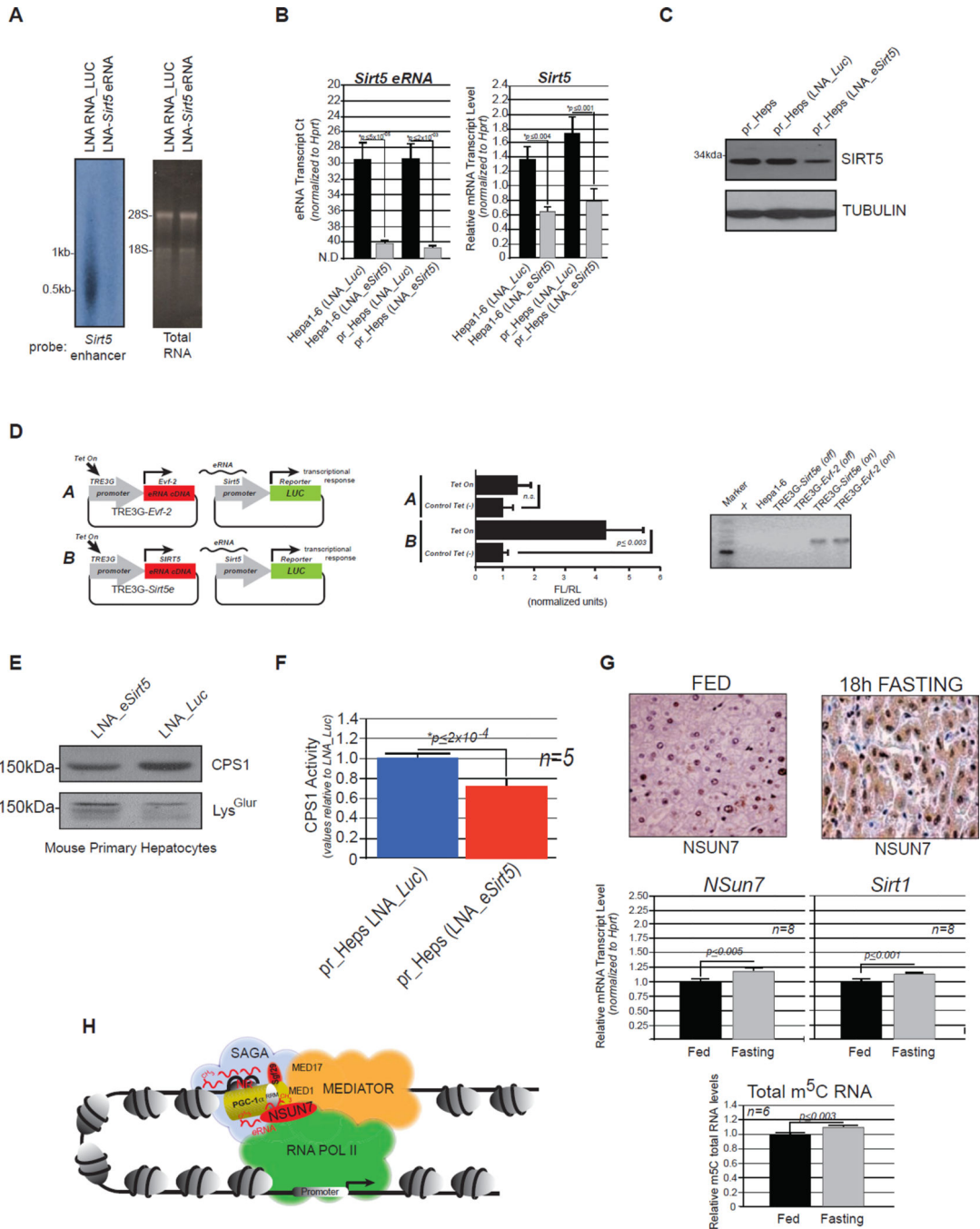


Figure 7. Physiological function of *Sirt5* eRNA

A) Northern blot analysis of *Sirt5* eRNAs in control and following eRNA depletion with antisense LNA RNAs (LNA-*Sirt5*) in mouse primary hepatocytes (left panel). Total RNA was visualized with ethidium bromide under UV transillumination (right panel). B) *Sirt5* eRNA (left panel) and mRNA (right panel) qPCR analysis in control and *Sirt5* eRNA-depleted Hepal-6 hepatoma cells and primary mouse hepatocytes. C) Western blot of SIRT5 in control and following depletion of the corresponding eRNAs in primary mouse hepatocytes. Tubulin was used as a loading control (lower panel). D) Schematics illustrating

Tet-On inducible promoter in TRE3G™ (Clontech) to drive transcription of *Evf-2* and *Sirt5* eRNAs, respectively (*left panel*). Graph showing the normalized luciferase activity of the *Sirt5* reporter co-transfected with TRE3G-Evf-2 or TRE3G-Sirt5 eRNA in the presence or absence of doxycycline as indicated. End-point PCR is shown for the Tet On abundance of *Sirt5* and *Evf-2* eRNAs, respectively. E) Immunoblots for total CPS1 (*upper panel*) and glutaryl-lysine CPS1 (*lower panel*) in control and *Sirt5* eRNA-depleted primary mouse hepatocytes. F) CPS1 enzyme activity was measure and normalized against the LNA control for luciferase. G) Immunohistochemical staining of NSUN7 from paraffin embedded liver sections from mice fed and fasted for 18 hours. qPCR analysis of *NSun7* and *Sirt1* mRNA of livers (large lobe) in control or fasted DBA mice (n=8). Enrichment of m⁵C-RNA was quantified by colorimetric analysis of m⁵C nuclear RNA following the same 18 hour fast. H) In our proposed model, upon PGC-1 α methylation by SET7/9, the interaction with SAGA and Mediator is reinforced. NSUN7 methylation of eRNAs associated with PGC-1 α target genes reinforces the stability of the eRNA-bound protein complex.